ISSN 1063-7826, Semiconductors, 2017, Vol. 51, No. 4, pp. 503–508. © Pleiades Publishing, Ltd., 2017.
Original Russian Text © G.B. Galiev, S.S. Pushkarev, A.M. Buriakov, V.R. Bilyk, E.D. Mishina, E.A. Klimov, I.S. Vasil'evskii, P.P. Maltsev, 2017, published in Fizika i Tekhnika Poluprovodnikov, 2017, Vol. 51, No. 4, pp. 529–534.

PHYSICS OF SEMICONDUCTOR DEVICES

Terahertz-Radiation Generation and Detection in Low-Temperature-Grown GaAs Epitaxial Films on GaAs (100) and (111)A Substrates

G. B. Galiev[a], S. S. Pushkarev[a]*, A. M. Buriakov[b], V. R. Bilyk[b], E. D. Mishina[b], E. A. Klimov[a], I. S. Vasil'evskii[c], and P. P. Maltsev[a]

[a] *Institute of Ultrahigh-Frequency Semiconductor Electronics, Russian Academy of Sciences, Moscow, 117105 Russia*
[b] *Moscow Technological University "MIREA", Moscow, 119454 Russia*
[c] *National Research Nuclear University "MEPhI", Moscow, 115409 Russia*
**e-mail: s_s_e_r_p@mail.ru*

Submitted September 20, 2016; accepted for publication September 26, 2016

Abstract—The efficiency of the generation and detection of terahertz radiation in the range up to 3 THz by LT-GaAs films containing equidistant Si doping δ layers and grown by molecular beam epitaxy on GaAs (100) and (111)Ga substrates is studied by terahertz spectroscopy. Microstrip photoconductive antennas are fabricated on the film surface. Terahertz radiation is generated by exposure of the antenna gap to femtosecond optical laser pulses. It is shown that the intensity of terahertz radiation from the photoconductive antenna on LT-GaAs/GaAs (111)Ga is twice as large as the intensity of a similar antenna on LT-GaAs/GaAs(100) and the sensitivity of the antenna on LT-GaAs/GaAs (111)Ga as a terahertz-radiation detector exceeds that of the antenna on LT-GaAs/GaAs(100) by a factor of 1.4.

DOI: 10.1134/S1063782617040054

1. INTRODUCTION

Time-resolution terahertz spectroscopy is a modern rapidly developing method for the diagnostics of various materials and biological objects using low-intensity terahertz-range (100 GHz–3 THz) electromagnetic radiation. In this method, terahertz radiation is generated and detected by photoconductive antennas (PC antennas) based on special semiconductor materials. Such materials should feature either a short pulse-relaxation time or short lifetime of photoexcited carriers. Materials of the first type are defect-free single-crystal GaAs films [1] and the materials of the second type are GaAs films grown by molecular-beam epitaxy at low substrate temperatures (LT-GaAs) [2].

Lowering of the growth temperature leads to the suppression of arsenic re-evaporation from the surface of the grown film and the latter traps up to 1.5 at % of excess arsenic (whereas the stoichiometric GaAs compound contains exactly 50% of Ga and 50% of As) [3–5]. Thus, the LT-GaAs film has a high concentration of As_{Ga} antistructural defects (As atoms at Ga atomic sites), on the order of 10^{20} cm^{-3}. In the charged state As^{+}_{Ga}, these defects behave as electron traps and, thus, ensure a very short (less than a picosecond) photoexcited-electron lifetime [7].

To increase the concentration of As^{+}_{Ga} charged defects, the LT-GaAs material is doped with an acceptor impurity (as a rule, beryllium) [7]. As was shown in [8, 9], LT-GaAs:Be structures can be used in optoelectronic devices operating in the terahertz-frequency range, which have better parameters as compared with devices based on undoped LT-GaAs. However, because of the high toxicity of beryllium, it is rarely used in molecular beam epitaxy (MBE) and is not widespread in production, since this requires additional safety measures. In addition, the presence of a Be source in MBE facilities enhances the background *p*-type impurity concentration, which negatively affects *n*-type heterostructures, e.g., HEMT heterostructures with a high electron mobility, grown in the facilities.

It is well-known that silicon exhibits pronounced amphoteric properties as a dopant in epitaxial GaAs films grown on GaAs substrates with the (111)Ga crystallographic orientation at standard growth temperatures (500–600°C). In this case, by changing the ratio γ between arsenic and gallium flows, one can grow Si-doped GaAs layers with *n*- or *p*-type conductivity [10, 11]. However, the doping properties of Si in the LT-GaAs films grown on GaAs (111)Ga substrates have not been investigated so far.

In this study, we investigate terahertz-radiation generation and detection by PC antennas on LT-GaAs films epitaxially grown on GaAs substrates with the standard (100) crystallographic orientation and with the (111)Ga orientation and doped with Si. The aim of

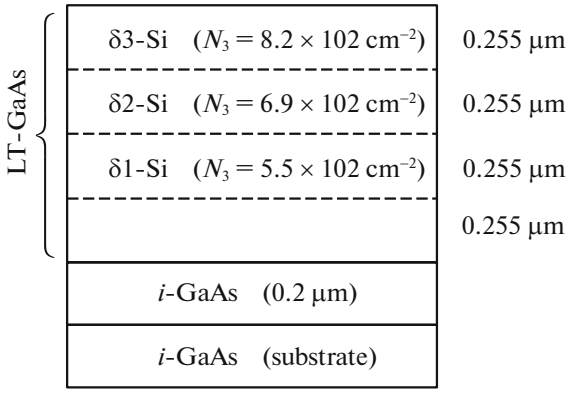

Fig. 1. Sample design.

this study is to establish which substrate ensures better characteristics of the LT-GaAs epitaxial films as materials for PC terahertz antennas. In this case, it is taken into account that the quality of the LT-GaAs film is affected not only by the amphoteric properties of Si atoms, but also by the features of the crystal structure acquired by the LT-GaAs film upon growth on different substrates. In addition, the properties of the investigated PC antennas are compared with those of the nonlinear ZnTe crystal traditionally used for the same purposes.

2. EXPERIMENTAL

The investigated samples of similar design were grown on semi-insulating GaAs (100) and (111)Ga substrates by MBE. Hereinafter, the sample on the GaAs(100) substrate is denoted as LT-GaAs/GaAs(100) (growth process no. 975-3.3) and the sample on the GaAs (111)Ga substrate, as LT-GaAs/GaAs(111)Ga (growth process no. 978-6.3). The sample design is illustrated in Fig. 1. The samples consist of two layers: an *i*-GaAs layer with a thickness of 0.2 μm grown at a temperature of 560°C and a LT-GaAs layer with a thickness of 1 μm grown at a temperature of 230°C. The LT-GaAs layer contains three Si δ layers at a distance of 0.255 μm from each other. The Si atomic concentration in each δ layer is presented in Fig. 1. The ratio between the As_4 and Ga flows during growth was ~20. The grown samples were annealed in the growth chamber of the MBE facility in an As_4 flow at a temperature of 590°C for one hour. The surface morphology, diffraction reflection curves, and photoluminescence spectra of these samples were discussed in [12].

The microstrip antennas were formed on the surface of the grown samples by photolithography. These antennas were Ti/Al (50/800 nm) ohmic contacts in the form of two parallel strips with a width of 100 μm and a distance of 200 μm between them (Fig. 2a).

A schematic representation of the experimental setup for studying terahertz-radiation generation and detection is shown in Fig. 2b. The optical pump source of the PC antennas was a solid-state laser based on a sapphire crystal doped with titanium ions which operated at a wavelength of 800 nm (the photon energy was 1.55 eV), a pulse length of 100 fs, and a pulse-repetition rate of 80 MHz. The average pump and probe power densities were 3.71×10^3 W/cm^2 and 0.88×10^3 W/cm^2, respectively. The optical pump radiation was focused to a spot ~12 μm in diameter between the PC antenna electrodes. To obtain the optimal conditions for terahertz-radiation generation, the pump beam spot was shifted toward the anode electrode of the PC antenna, since the electric field between two distant metal linear electrodes is highly inhomogeneous and concentrated near the anode [13, 14].

The same fabricated samples of PC antennas on the LT-GaAs (100) and LT-GaAs (111)Ga films were tested in the terahertz-radiation generation and detection modes. A nonlinear ZnTe crystal served as a ref-

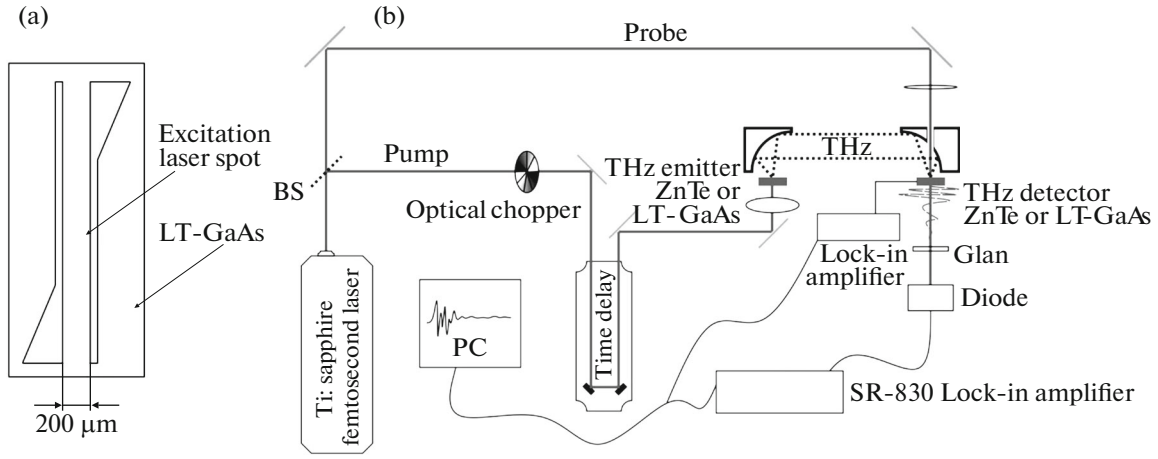

Fig. 2. Schematic representation of (a) the PC antennas on LT-GaAs and (b) experimental setup for the generation and detection of terahertz radiation from the nonlinear ZnTe crystal.

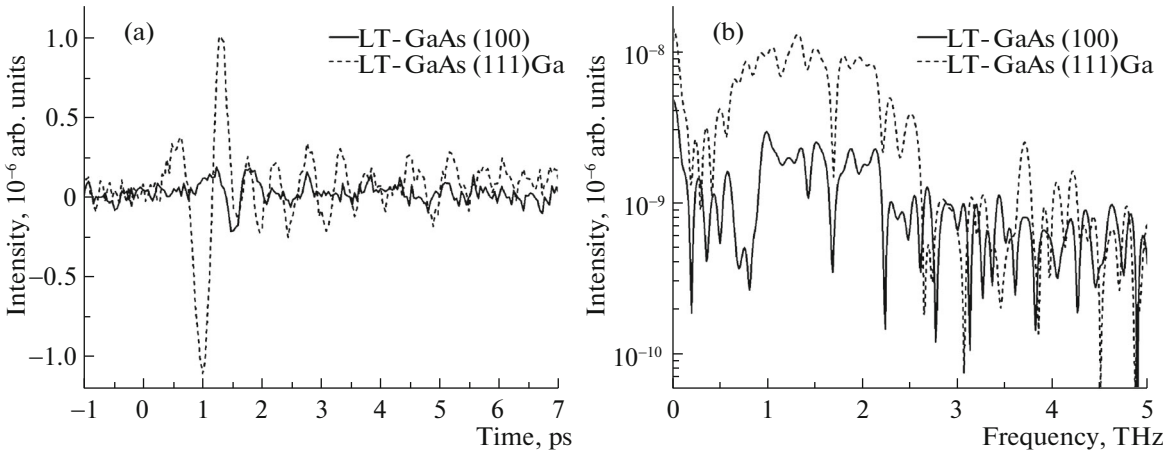

Fig. 3. Terahertz-radiation generation by the LT-GaAs films without external electric field (the ZnTe crystal is a detector). (a) Time dependence of terahertz radiation from the LT-GaAs (100) and (111)Ga films; (b) frequency spectrum of the terahertz radiation.

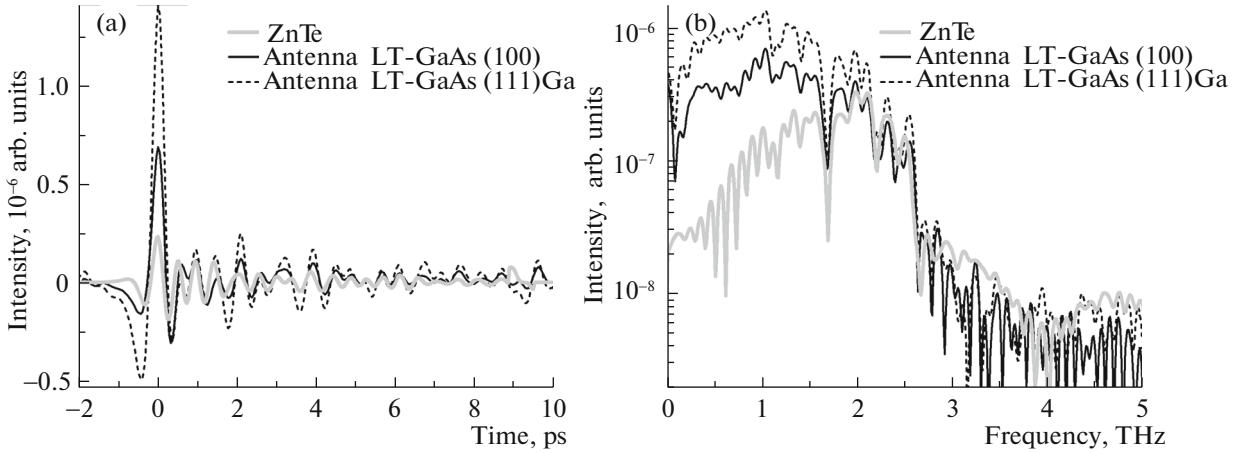

Fig. 4. Comparison of terahertz generators (with a ZnTe crystal as a detector). (a) Time shape of the terahertz pulse at a bias voltage of 75 V and (b) terahertz-radiation spectrum.

erence generator and detector. During terahertz-radiation generation by the PC antennas, a bias voltage was applied to their contacts, which induced an electric field in the gap between the contacts, and accelerated photoexcited carriers. The bias was varied in the range of 0–60 V. During terahertz-radiation detection by the PC antennas, a bias voltage was not applied and the photocurrent in the antenna was induced by the electric field of terahertz radiation affecting photoexcited carriers. This photocurrent was a terahertz electric signal fully corresponding to the detected terahertz pulse. To measure this signal, we used an SR 830 synchronous amplifier, which allows the extraction of a signal of specified wavelength from the noisy medium (even when the noise and signal are indistinguishable in the time domain, but the signal has a certain frequency range and there are no large noise peaks within this range, the noise and signal can be separated).

In the circuit with the nonlinear-optical ZnTe crystal, terahertz-radiation detection is based on electro-optical gating of a broad terahertz pulse by short femtosecond pulses [15, 16]. The operating principle is based on the interaction between terahertz and optical radiation in the nonlinear medium by means of modulation of the optical radiation phase by a terahertz wave. The terahertz-wave phase is scanned using the time delay line. Nonlinear crystals with high second-order nonlinear susceptibility ($LiTaO_3$, $LiNbO_3$, and ZnTe) are used as detectors and generators [14].

3. RESULTS AND DISCUSSION

Figure 3 shows the time shapes and frequency spectra of terahertz radiation from the PC antennas without applying voltage to their contacts. The ZnTe crystal was used as a detector. In this case, the tera-

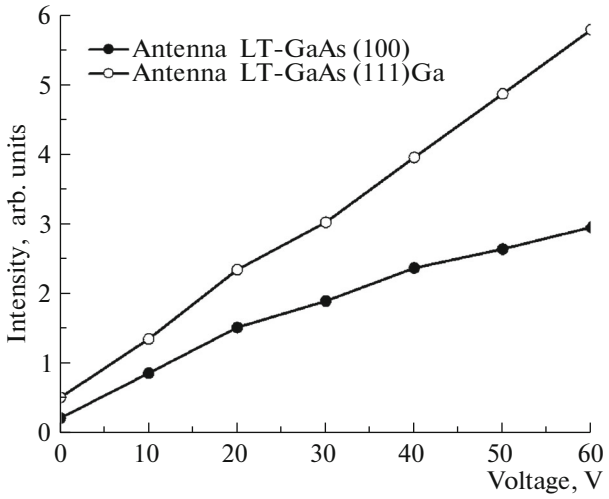

Fig. 5. Bias-voltage dependence of the antenna radiation intensity normalized to the ZnTe radiation intensity.

hertz radiation was generated by photoexcited charge carriers, which were accelerated by internal electric fields in the LT-GaAs film. The spectra of the generated terahertz radiation are similar for both films; however, the spectral intensity of the LT-GaAs (111)Ga film is higher by an order of magnitude. In zero applied electric field, the LT-GaAs (100) and LT-GaAs (111)Ga films generate terahertz radiation with an intensity lower by one–two orders of magnitude than that generated by the nonlinear ZnTe crystal. The frequency of ~0.1 THz in the spectrum corresponds to the noise background. It should be noted that water vapor lowers the setup sensitivity near the absorption lines. At a frequency of 1.67 THz, there is a small dip in the spectrum, which corresponds to intense absorption by water vapor.

When a bias voltage of 60 V was applied to the PC antenna contacts, the intensity of terahertz-radiation generation relative to the zero-bias intensity increased by a factor of 164 for the PC antenna on LT-GaAs (100) and 90 for the PC antenna on LT-GaAs (111)Ga. Figure 4 shows the time shapes and frequency spectra of terahertz radiation from the PC antennas at a bias voltage of 60 V. It can be seen that the intensity of radiation of the PC antenna on LT-GaAs (111)Ga is twice as much as that of the PC antenna on LT-GaAs (100). The radiation spectra of the PC antennas are similar; their maxima are near 1 THz, while the spectral maximum of ZnTe crystal radiation is shifted toward higher frequencies and lies near 2 THz. In addition, the width of the generated terahertz spectrum in the case of LT-GaAs is larger for samples of both types.

The bias-voltage dependence of the intensity of terahertz radiation from the PC antennas is presented in Fig. 5. A significant increase in intensity is observed for the PC antenna on LT-GaAs (111)Ga. This growth is related to a higher photocurrent caused by a higher free carrier density in the LT-GaAs (111)Ga film. In addition, the bias-voltage dependence of the terahertz-radiation intensity for the antenna on LT-GaAs (100) is sublinear, while in the case of the antenna on LT-GaAs (111)Ga it is almost linear.

In addition, we investigated the detection properties of the PC antennas on LT-GaAs (100) and LT-GaAs (111)Ga. Terahertz radiation was generated by the nonlinear ZnTe crystal. Figure 6 shows the time shapes and frequency spectra of the terahertz electric pulses measured by the PC antennas. It is established that the sensitivity of the PC antenna on LT-GaAs (111)Ga exceeds that of the PC antenna on LT-GaAs (100) and nonlinear ZnTe crystal by a factor of 1.5. In addition, it can be seen that the total width of the electrical-signal spectrum is 3 THz for all the detectors. However, in the spectrum of the signal measured by the nonlinear ZnTe crystal, the frequency range near

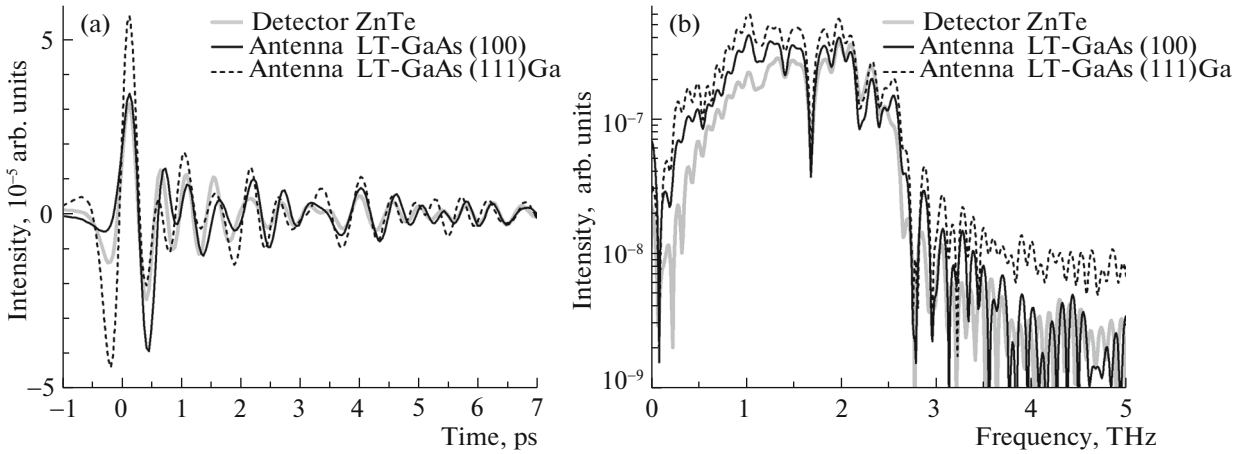

Fig. 6. Comparison of terahertz detectors (with a ZnTe crystal as a terahertz-radiation generator). (a) Time shape of the electric pulse from detectors of three types and (b) frequency spectrum of the electric pulse from detectors of three types.

Characteristics of the nonlinear ZnTe crystal, films, and PC antennas at an applied voltage of 75 V in the frequency range of 0–5 THz

	ZnTe	LT-GaAs film		PC antenna on LT-GaAs	
		GaAs (100) substrate	GaAs (111)Ga substrate	GaAs (100) substrate	GaAs (111)Ga substrate
Generation					
$(f_{1/2})_{min}$, THz	1.00	~0.5**	0.60	0.42	0.28
$(f_{1/2})_{max}$, THz	2.37	~3.5**	2.17	1.97	1.58
Radiation band, THz	1.37	~3.0**	1.57	1.55	1.30
Normalized integrated THz radiation intensity	1	~0.0014**	0.050	2.30	4.52
Detection					
$(f_{1/2})_{min}$, THz	1.03	–	–	0.83	0.81
$(f_{1/2})_{max}$, THz	2.32	–	–	2.13	2.13
Radiation band, THz	1.29	–	–	1.30	1.32
Normalized integrated THz radiation intensity	1	–	–	1.28	1.80

*The frequency determination error is ±0.04 THz. **The given values are just estimated, since the low signal intensity made it difficult to analyze its spectrum.

2 THz is relatively more intense, while the spectrum of the signals measured by the PC antennas contains an additional high-intensity region near 1 THz, which makes the signal more uniform.

The low-frequency region in the radiation and sensitivity spectra of the PC antennas can be related to their topology: the antenna in the form of two parallel strip contacts with distance d between them is resonant and its resonance frequency is determined by the expression

$$d = \frac{\lambda}{2\sqrt{\varepsilon_{eff}}}, \quad \varepsilon_{eff} = \frac{\varepsilon_{GaAs} + 1}{2} = 7$$

and amounts to 0.28 THz. Nevertheless, as was shown in [14], the radiation spectra of microstrip PC antennas do not contain sharp peaks corresponding to resonance frequencies. With a change in the PC antenna sizes, the spectrum only slightly changes its shape.

A more thorough analysis of all the investigated spectra presented in Figs. 3b, 4b, and 6b yielded the numerical spectral characteristics listed in the table. The radiation/sensitivity band was determined as a frequency band where 50% of the integral power (71% of the integral intensity) is radiated/detected, while the intensities at the threshold frequencies $(f_{1/2})_{min}$ and $(f_{1/2})_{max}$ are almost the same.

4. CONCLUSIONS

In this study, we showed that LT-GaAs films on GaAs (100) and (111)Ga substrates generate terahertz radiation in the range of up to 3 THz upon their exposure to femtosecond laser pulses with a wavelength of 800 nm. Comparison of the films shows that the intensity of terahertz radiation from the LT-GaAs film on the nonsingular GaAs (111)Ga substrate exceeds that from the LT-GaAs film on the singular GaAs (100) substrate by a factor of 3.4. The intensity of terahertz radiation from the PC antenna in the form of two parallel Ti/Au strips with a width of 100 μm and a distance of 200 μm between them formed on the surface of these films at a voltage of 60 V applied to the antenna contacts is twice as large as the intensity of terahertz radiation from the corresponding films without antennas. Comparison of the PC antennas shows that the intensity of terahertz radiation from the PC antenna on LT-GaAs/GaAs (111)Ga is twice as large as the intensity for the same antenna on LT-GaAs/GaAs (100) and is higher than the intensity of terahertz radiation from the nonlinear ZnTe crystal by a factor of 4.5.

The sensitivity of the PC antenna on LT-GaAs/GaAs (111)Ga operating as a terahertz-radiation detector exceeds that of the PC antenna on LT-GaAs/GaAs (100) and nonlinear ZnTe crystal by factors of 1.4 and 1.8, respectively.

The PC antenna on LT-GaAs/GaAs (111)Ga operating as a terahertz-radiation generator is much better than the PC antenna on LT-GaAs/GaAs (100). At the same time, the PC antenna on LT-GaAs/GaAs (111)Ga operating as a terahertz-radiation detector is only slightly better than the PC antenna on LT-GaAs/GaAs (100).

Thus, the better characteristics of the PC antennas on LT-GaAs films on the (111)Ga substrates as com-

pared to those of the antennas on LT-GaAs films on the (100) substrates should be attributed to the features of the crystal structure of the LT-GaAs epitaxial films formed on the nonsingular GaAs (111)Ga substrate.

ACKNOWLEDGMENTS

This study was supported by the Russian Science Foundation (agreement no.14-12-01080), Ministry of Education and Science of the Russian Federation (subsidy agreement no. 14.Z50.31.0034), and the Russian Foundation for Basic Research (project no. 16-29-03294 ofi_m).

REFERENCES

1. M. Venkatesh, K. S. Rao, T. S. Abhilash, S. P. Tewari, and A. K. Chaudhary, Opt. Mater. **36**, 596 (2014).
2. G. B. Galiev, E. A. Klimov, D. V. Lavrukhin, A. E. Yachmenev, R. R. Galiev, D. S. Ponomarev, R. A. Khabibullin, Yu. V. Fedorov, A. S. Bugaev, Nano-Mikrosist. Tekh. **6**, 28 (2014).
3. Z. Liliental-Weber, W. Swider, K. M. Yu, J. Kortright, F. W. Smith, and A. R. Calawa, Appl. Phys. Lett. **58**, 2153 (1991).
4. Z. Liliental-Weber, H. J. Cheng, S. Gupta, J. Whitaker, K. Nichols, and F. W. Smith, J. Electron. Mater. **22**, 1465 (1993).
5. M. Missous, Microelectron. J. **27**, 393 (1996).
6. B. Grandidier, Huajie Chen, R. M. Feenstra, D. T. McInturff, P. W. Juodawlkis, and S. E. Ralph, Appl. Phys. Lett. **74**, 1439 (1999).
7. Toshihiko Ouchi and Kousuke Kajiki, US Patent No. 8835853 (2014).
8. J.-L. Coutaz, J.-F. Roux, A. Gaarder, S. Marcinkevicius, J. Jasinski, K. Korona, M. Kaminska, K. Bertulis, and A. Krotkus, in *Proceedings of the 11th International Semiconducting and Insulating Material Conference, Canberra, Australia, July 3–7, 2000*, p. 89.
9. P. Specht, S. Jeong, H. Sohn, M. Luysberg, A. Prasad, J. Gebauer, R. Krause-Rehberg, and E. R. Weber, Mater. Sci. Forum **258–263**, 251 (1997).
10. G. B. Galiev, V. G. Mokerov, V. V. Saraikin, Yu. V. Slepnev, G. I. Shagimuratov, R. M. Imamov, and E. M. Pashaev, Tech. Phys. **46**, 411 (2001).
11. G. Galiev, V. Kaminskii, D. Milovzorov, L. Velihovskii, and V. Mokerov, Semicond. Sci. Technol. **17**, 120 (2002).
12. G. B. Galiev, E. A. Klimov, M. M. Grekhov, S. S. Pushkarev, D. V. Lavrukhin, and P. P. Maltsev, Semiconductors **50**, 195 (2016).
13. P. Uhd Jepsen, R. H. Jacobsen, and S. R. Keiding, J. Opt. Soc. Am. B **13**, 2424 (1996).
14. Masahiko Tani, Shuji Matsuura, Kiyomi Sakai, and Shinichi Nakashima, Appl. Opt. **36**, 7853 (1997).
15. S. P. Kovalev and G. Kh. Kitaeva, JETP Lett. **94**, 95 (2011).
16. C. Winnewisser, P. Uhd Jepsen, M. Schall, V. Schyja, and H. Helm, Appl. Phys. Lett. **70**, 3069 (1997).

Translated by E. Bondareva